Nitrogen Fixation Hot Paper

How to cite: *Angew. Chem. Int. Ed.* **2021**, *60*, 25804–25808
International Edition: doi.org/10.1002/anie.202111325
German Edition: doi.org/10.1002/ange.202111325

Molybdenum-Mediated N_2-Splitting and Functionalization in the Presence of a Coordinated Alkyne

*Hannah K. Wagner, Hubert Wadepohl, and Joachim Ballmann**

Abstract: *A new [PCCP]-coordinated molybdenum platform comprising a coordinated alkyne was employed for the cleavage of molecular dinitrogen. The coordinated η^2-alkyne was left unaffected during this reduction. DFT calculations suggest that the reaction proceeds via an initially generated terminal N_2-complex, which is converted to a dinuclear μ-(η^1:η^1)-N_2-bridged intermediate prior to N–N bond cleavage. Protonation, alkylation and acylation of the resulting molybdenum nitrido complex led to the corresponding N-functionalized imido complexes. Upon oxidation of the N-acylated imido derivative in MeCN, a fumaronitrile fragment was built up via C–C coupling of MeCN to afford a dinuclear molybdenum complex. The key finding that the strong N≡N bond may be cleaved in the presence of a weaker, but spatially constrained C≡C bond contradicts the widespread paradigm that coordinated alkynes are in general more reactive than gaseous N_2.*

In 1995, the direct cleavage of N_2 to afford two Mo^{VI}-nitrido complexes was first achieved by Cummins and co-workers starting from a trigonal Mo^{III}-trisanilide.[1] In the following years, similar (in part heterobimetallic) trisanilides and related trigonal molybdenum complexes (e.g. Mes_3Mo) were developed[2] and shown to split N_2 as well,[3] while Schrock and co-workers demonstrated that this challenging transformation may also be accomplished using a POCOP-molybdenum pincer complex with a tetragonally coordinated molybdenum center.[4] Nishibayashi,[5] Schneider[6] and Mézailles[7] augmented and advanced this approach by employing different octahedral or square pyramidal PNP-, P(NH)P- and PPP-molybdenum precursors for the cleavage of N_2, which underlines the importance of Schrock's finding in retrospective.

Very recently, yet another breakthrough has been reported on the basis of Schrock's anionic nitrido complex $[(POCOP)Mo(N)I]^-$,[4] which is generated upon reductive N_2-cleavage: Mézailles and co-workers have found that the corresponding $1e^-$-oxidized Mo^V nitride (POCOP)Mo(N)I reacts with alkynes (in the presence of $TlBAr_F$) to produce an organic nitrile.[8] Although the latter product was obtained in 24% yield (GC) only, it was shown that a N_2-derived nitride may undergo [2+2] cycloadditions, which marks an important milestone on the path to atom-efficient syntheses of *N*-containing fine chemicals starting from N_2 and alkynes.[9] At present, these elusive processes can only be envisioned in a stoichiometric fashion as a catalytic process would require the presence of an alkyne during N_2-splitting. However, the relative bond strength orders (RBSOs) of alkynes (approx. 2.4) and N_2 (3.04) suggest that alkynes are more easily activated than free N_2,[10] which raises the pressing question whether direct N_2-cleavage is feasible in the presence of an alkyne at all.

Herein, a diiodo molybdenum complex featuring a η^2-alkyne was reduced under N_2 and shown to split molecular dinitrogen, while the ligand's alkyne unit remained (chemically) unaltered. Hence, the widespread paradigm that alkynes are more easily reduced than N_2 was contradicted, albeit under the precondition that a spatially and rotationally constrained alkyne is used.

To begin with, $MoI_3(thf)_3$ was reacted with 2,2′-($^iPr_2P$)$_2$-substituted tolane in the presence of Sn^0 powder to afford the molybdenum diiodo complex **1** in 70% yield (see Scheme 1).[11] In the crystallographically determined molecular structure of **1**, a strongly coordinated alkyne[12] ($4e^-$ donor, $\delta(^{13}C\{^1H\}) = 221.1$ ppm) with a C13–C14 bond length of 1.32 Å is found (see Figure 1), suggesting that a metallacyclopropene resonance structure (see inset in Scheme 1) is well-suited to describe the alkyne-Mo interaction. Reduction of **1** ($\delta(^{31}P\{^1H\}) = 60.4$ ppm) with Na/Pb alloy (10 weight-% Na, 1.2 equiv) in the presence of N_2 (1 atm) at r.t. led to the formation of the corresponding Mo nitride **2** ($\delta(^{31}P\{^1H\}) = 68.0$ ppm), which was isolated as a beige powder in 95% yield.

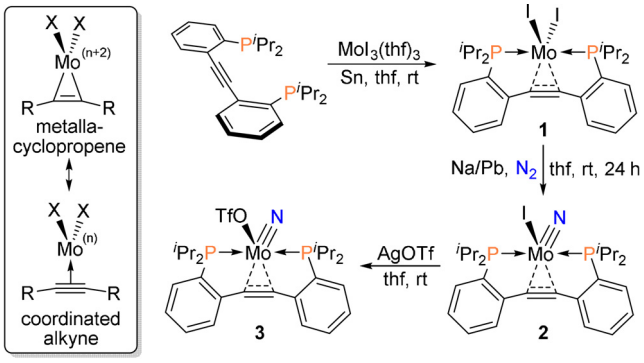

Scheme 1. Synthesis and resonance structures (inset) of complexes **1**–**3**.

[*] H. K. Wagner, Prof. Dr. H. Wadepohl, Priv. Doz. Dr. J. Ballmann
Anorganisch-Chemisches Institut, Universität Heidelberg
Im Neuenheimer Feld 276, 69120 Heidelberg (Germany)
E-mail: Joachim.ballmann@uni-heidelberg.de
Supporting information and the ORCID identification number(s) for the author(s) of this article can be found under: https://doi.org/10.1002/anie.202111325.

© 2021 The Authors. Angewandte Chemie International Edition published by Wiley-VCH GmbH. This is an open access article under the terms of the Creative Commons Attribution Non-Commercial License, which permits use, distribution and reproduction in any medium, provided the original work is properly cited and is not used for commercial purposes.

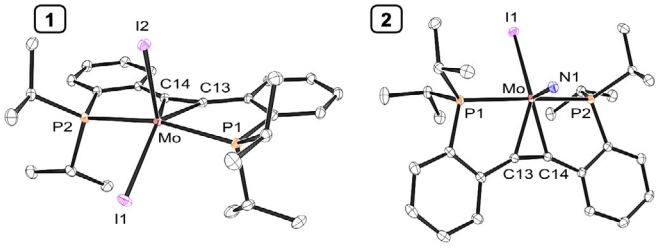

Figure 1. ORTEP plots of the molecular structures of **1** and **2** (see Supporting Information for details).

To confirm that the nitrido moiety in **2** indeed originates from molecular dinitrogen, the corresponding ^{15}N-labeled complex **2-^{15}N** was prepared from $(^{15}N)_2$ and the nitride resonance detected in the $^{15}N\{^1H\}$ NMR spectrum at $\delta =$ 825 ppm. Single crystal X-ray diffraction confirmed the presence of a Mo≡N moiety (d(Mo–N1) = 1.66 Å) in **2** with N1 occupying the apical position of the distorted square pyramidal coordination polyhedron around the Mo core (see Figure 1).[11] In difference to **1** ($\nu_{C\equiv C} = 1734\ cm^{-1}$), the coordinated alkyne in **2** ($\nu_{C\equiv C} = 1863\ cm^{-1}$) is best described as 2 e$^-$ donor ($\delta(^{13}C\{^1H\}) = 132.1$ ppm),[12] which is also reflected by the slightly shorter C13–C14 bond length of 1.28 Å in **2** (compared to **1**). Hence, a certain degree of ligand non-innocence is evident for these complexes.[13] The η^2-alkyne in the corresponding triflate **3** (prepared according to Scheme 1), is also interpreted as a 2 e$^-$ donor ($\delta(^{13}C\{^1H\}) =$ 132.2 ppm), indicating that **2** and **3** are both well described as Mo^{IV} nitrides.

To gain first insights into the conversion of **1** to **2**, the reaction progress was monitored by variable-temperature $^{31}P\{^1H\}$ NMR spectroscopy. Between −40 °C and −10 °C, the $^{31}P\{^1H\}$ NMR signal of **1** steadily decreased, but no other signals appeared, that is, one or more NMR-silent intermediates were formed. At approximately 5 °C, the formation to **2** set in and is completed within 24 h at 20 °C. Given that all our attempts to isolate the intermediate(s) met with failure, we turned our attention to CO derivatives as model compounds. As expected, CO was found to readily react with **1** to afford the corresponding CO complex (see Supporting Information), which was then reduced with KC_8 either under N_2 or under argon. In both cases (N_2 or Ar), lustrous dark crystals were isolated in 95 % yield and unambiguously identified as compound **4** by single crystal X-ray diffraction (see Figure 2).

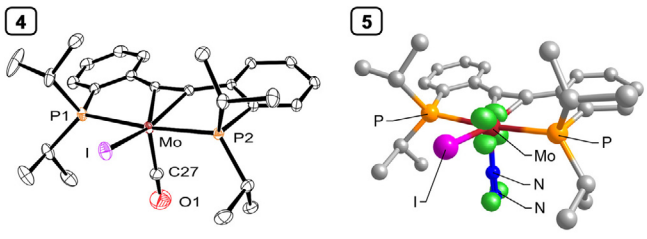

Figure 2. ORTEP plot of the molecular structure of **4** (see Supporting Information for details) and Mulliken spin density plot of **5** (from NEVPT2-CASSCF(13,13) calculations with the geometry of **5** optimized on the PBE0/Def2-TZVP(RI) level of theory, incl. GD3 and CPCM$_{thf}$, see Supporting Information for details).

An effective magnetic moment of $\mu_{eff} = 1.59\ \mu_B$ was determined (Evans method) for solutions of **4** in thf-d_8, indicative of an $S = {}^1/_2$ ground state. On basis of these results, the corresponding terminal N_2-complex **5** is proposed as one of the first intermediates in the reduction of **1** under N_2 (see Scheme 2).

DFT modelling studies (PBE0/Def2-TZVP(RI) level of theory) are in line with the proposed structure and the expected $S = {}^1/_2$ ground state of **5**, while dissociation of N_2 was observed upon optimization of the corresponding quartet state in silico. According to NEVPT2-CASSCF and Mulliken spin density analysis, the unpaired electron in **5** is mostly located on the metal (approx. 70 %) and the distal nitrogen atom (approx. 30 %) of the N_2 ligand (see Figure 2).

Once **5** is formed, its dimerization (with loss of N_2) affords the μ-(η^1:η^1)-N_2-bridged intermediate ^{3}**6** in its triplet ground state.[14] In the calculated structure of ^{3}**6** (PBE/Def2-TZVP-(RI-J), GD3, gCP, CPCM$_{thf}$) the two [PCCP]MoI fragments are mutually twisted by approx. 90° (dihedral angle I–Mo···Mo–I = 93°) and interconnected by a nearly linear N_2 unit with $d_{N=N} = 1.19$ Å. A low-lying minimum energy crossing point (MECP) for the transition to the corresponding singlet state (^{1}**6**, $d_{N=N} = 1.20$ Å) was found and the singlet state was calculated to be higher in energy by only 5.0 kcal mol^{-1}. On basis of the $\delta^4\pi^{10}$-model[15] for bimetallic μ-(η^1:η^1)-N_2-bridged complexes with two square pyramidal metal ions, N_2-splitting is to be expected for **6** (2 × d^5-configured Mo^I + 4π electrons for the N_2 unit). Relaxed potential energy surface scans along the N–N bond of ^{3}**6** and ^{1}**6** revealed that the crucial N_2-cleavage step occurs on the singlet surface (see Supporting Information). The activation barrier associated with the zig-zag-type[1b] transition state (^{1}**TS**, $d_{N-N} = 1.64$ Å, $\Delta G^{\ddagger} = 26$ kcal mol^{-1} relative to ^{3}**6**, see Figure 3) is in line with the experimental observations, albeit at the upper ΔG limit.[16] Ultimately, two molecules of **2** are formed in an overall exergonic reaction ($\Delta G_r = -19.8$ kcal mol^{-1} relative to ^{3}**6**).

Although **2** may be directly functionalized at its nitrogen atom, it was found that the corresponding triflate **3** (see Scheme 1) reacts more readily, supposedly due to facile dissociation of the TfO$^-$ anion. A similarly enhanced reactivity has been reported upon addition of KOTf to POCOP-coordinated nitrido molybdenum iodides.[8] Hence, **3**

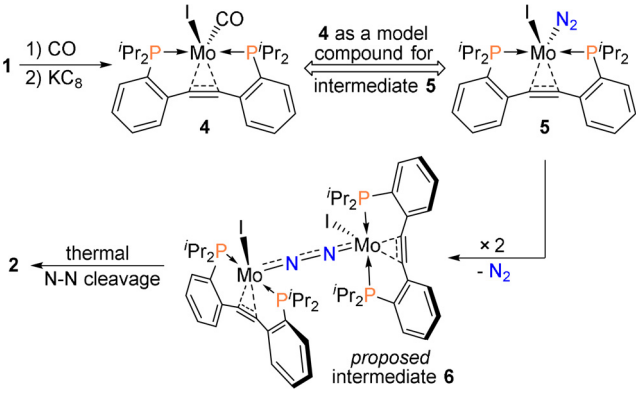

Scheme 2. Complex **4** as a model for **5** together with the proposed structure of intermediate **6**.

 © 2021 The Authors. Angewandte Chemie International Edition published by Wiley-VCH GmbH

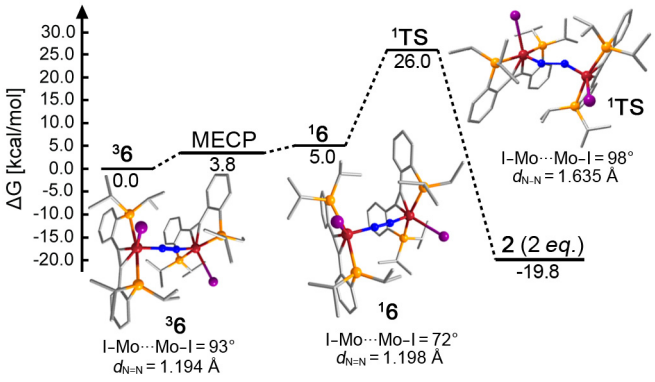

Figure 3. Calculated (PBE/Def2-TZVP(RI-J), GD3, gCP, $CPCM_{thf}$) Gibbs free energy profile for the conversion of ^{3}**6** to **2** (see Supporting Information for details).

was employed in the following and at first reacted with *tert*-butyl isonitrile to afford [**7**][OTf] as a beige salt (see Scheme 3 and Figure 4). The observation that the isonitrile merely coordinates to the Mo core is in line with the presence of a nucleophilic nitride and an electrophilic metal center.[17] This notion was then exploited by reacting **3** with different electrophiles (HCl, MeOTf and Ph(CO)Cl), which led to the expected *N*-functionalized imido complexes **8**, **9** and [**10**][OTf], respectively (see Scheme 3 and Figure 4).

For the preparation of the parent imido complex **8**, **3** was protonated (via reaction with HCl) and the resulting chloro complex then converted to the corresponding triflate via reaction with AgOTf (see Scheme 3). The ^{1}H NMR resonance of the N-H moiety in **8** was detected at $\delta(^1H) = 6.75$ ppm and identified in the ^{1}H-^{15}N HMBC NMR spectrum as a ^{15}N-coupled doublet ($^1J_{N,H} = 79$ Hz) with $\delta(^{15}N) = 73.2$ ppm. Starting from **3** and MeOTf, the *N*-methyl-imido derivative **9** was obtained and crystallized from CH_2Cl_2/pentane.[11] An analysis by single crystal X-ray diffraction revealed that **8** and **9** adopt fairly similar octahedral structures with the triflates coordinated to the Mo core in both cases (see Figure 4).

In contrast, a square pyramidal coordination environment was established for the corresponding *N*-benzoyl derivative

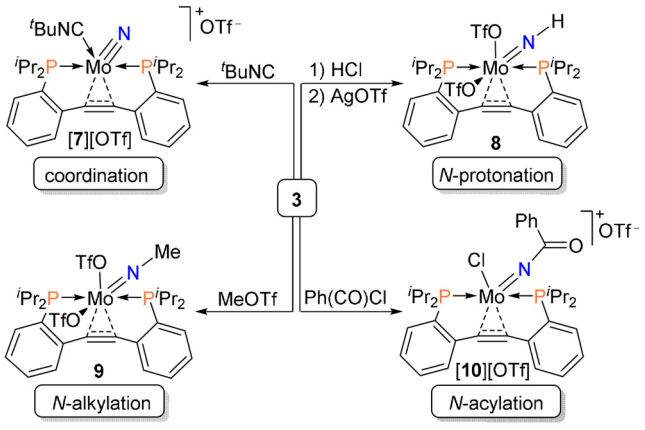

Scheme 3. Synthesis of [**7**][OTf], **8**, **9** and [**10**][OTf] starting from **3**.

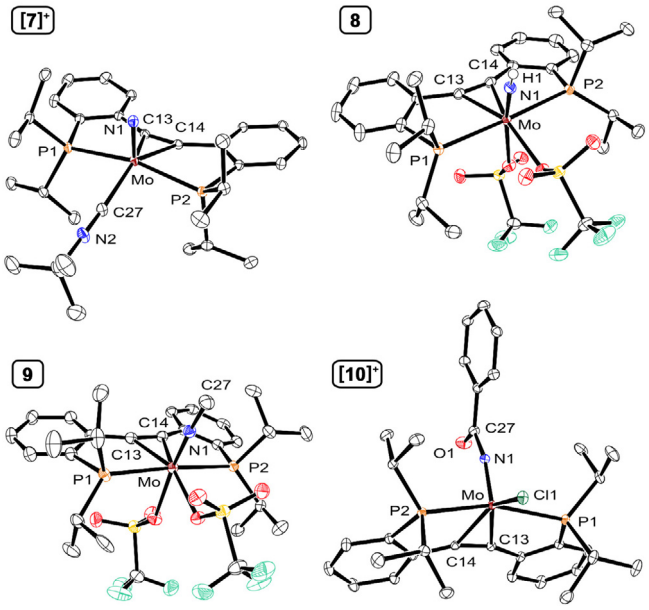

Figure 4. ORTEP plots of the molecular structures of [**7**]$^+$, **8**, **9** and [**10**]$^+$ (see Supporting Information for details).

[**10**]$^+$, which was crystallized as a cation with a non-coordinating triflate anion (see Scheme 3 and Figure 4). Nearly identical Mo = N bond lengths of 1.71 ± 0.01 Å have been found for all three imido complexes, supposedly due to the negligible *trans*-influence of the coordinated triflates in **8** and **9**.

The finding that the coordinated alkyne remained unsubstituted over the course of the former reactions, is also considered noteworthy. Preliminary experiments indicate that this holds true for the corresponding reactions of **3** with Me_3SiCl and EtI, although the resulting *N*-functionalized products have only been observed by NMR spectroscopy so far (see Supporting Information). Nishibayashi, Schneider, Cummins and others demonstrated that NH_3, $N(SiMe_3)_3$, MeCN or PhCN may be generated and released from related (*N*-H)-, (*N*-$SiMe_3$)-, (*N*-Et)- or (*N*-C(O)Ph)-functionalized molybdenum imido complexes, either in a catalytic (NH_3, $N(SiMe_3)_3$)[5] or in a stoichiometric fashion (MeCN, PhCN).[18] In a first screening for related stoichiometric follow-up functionalization reactions, a particularly remarkable transformation was discovered when [**10**][OTf] was reacted with *trans*-2,3-epoxybutane in MeCN. After 3d at 60 °C, a deep blue product was isolated from the reaction mixture and identified as [**11**][$OTf]_2$ (see Scheme 4).

In the ^{1}H NMR spectrum of [**11**][$OTf]_2$, the signals of the olefinic protons and the signal of the N-H protons were detected at $\delta = 5.65$ and 9.85 ppm, respectively. As expected, these ^{1}H NMR resonances were absent when the synthesis was repeated in MeCN-d_3. The presence of the central fumaronitrile linker in [**11**]$^{2+}$ was unambiguously confirmed by single crystal X-ray diffraction, although the corresponding singly deprotonated monocation [**11-H**]$^+$ was crystallized in form of its triflate salt (see Supporting Information for details). Mechanistically, it seems that the latter fumaronitrile is generated via C–C coupling of two MeCN ligands.[19] Given

 © 2021 The Authors. Angewandte Chemie International Edition published by Wiley-VCH GmbH

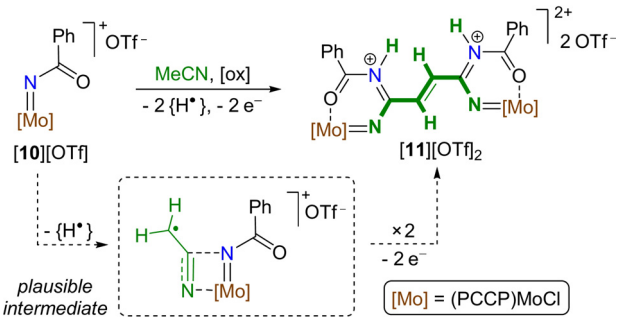

Scheme 4. C–C Coupling of two MeCN ligands to afford [**11**][OTf]$_2$ starting from [**10**][OTf].

that no reaction between [**10**][OTf] and MeCN is observed in the absence of an oxidant,[20] it is proposed that an H atom is oxidatively abstracted from a coordinated MeCN ligand[21] in the first step of the reaction. Supposedly, the *N*-benzoyl imido unit is then transferred to the nitrile carbon atom in a subsequent [2+2] cycloaddition step. The thus formed resonance stabilized radical is thought to dimerize in a consecutive step, although the latter two steps may as well occur in reverse order. The final product [**11**]$^{2+}$ is then generated via 2 e$^-$-oxidation (see Scheme 4).

In summary, it was shown that N_2 may be cleaved in the presence of a spatially and rotationally restricted η^2-alkyne unit, which demonstrates that alkyne reduction is not necessarily preferred over N_2 reduction. The latter alkyne also remained unaffected upon *N*-functionalization of **3** and upon treatment of [**10**][OTf] with oxidants, which warrants for further studies with this robust[20d] pincer framework.

Acknowledgements

This work was funded by the German Research Foundation (DFG grant BA 4859/2-1). The computational studies were supported by the state of Baden-Württemberg through bwHPC and the DFG through grant INST 40/467-1 FUGG (JUSTUS cluster). We thank Prof. Dr. Lutz H. Gade for generous support. Open Access funding enabled and organized by Projekt DEAL.

Conflict of Interest

The authors declare no conflict of interest.

Keywords: molybdenum · *N*-functionalization · nitrides · nitrogen fixation · phosphino alkyne ligands

[1] a) C. E. Laplaza, C. C. Cummins, *Science* **1995**, *268*, 861–863; b) C. E. Laplaza, M. J. A. Johnson, J. C. Peters, A. L. Odom, E. Kim, C. C. Cummins, G. N. George, I. J. Pickering, *J. Am. Chem. Soc.* **1996**, *118*, 8623–8638; c) J. C. Peters, J.-P. F. Cherry, J. C. Thomas, L. Baraldo, D. J. Mindiola, W. M. Davis, C. C. Cummins, *J. Am. Chem. Soc.* **1999**, *121*, 10053–10067; d) J. J. Curley, T. R. Cook, S. Y. Reece, P. Müller, C. C. Cummins, *J. Am. Chem. Soc.* **2008**, *130*, 9394–9405.

[2] a) D. J. Mindiola, K. Meyer, J.-P. F. Cherry, T. A. Baker, C. C. Cummins, *Organometallics* **2000**, *19*, 1622–1624; b) E. Solari, C. Da Silva, B. Iacono, J. Hesschenbrouck, C. Rizzoli, R. Scopelliti, C. Floriani, *Angew. Chem. Int. Ed.* **2001**, *40*, 3907–3909; *Angew. Chem.* **2001**, *113*, 4025–4027; c) M. Pucino, F. Allouche, C. P. Gordon, M. Wörle, V. Mougel, C. Copéret, *Chem. Sci.* **2019**, *10*, 6362–6367.

[3] For recent reviews, see: a) R. J. Burford, M. D. Fryzuk, *Nat. Rev. Chem.* **2017**, *1*, 0026; b) V. Krewald, *Dalton Trans.* **2018**, *47*, 10320–10329; c) N. Stucke, B. M. Flöser, T. Weyrich, F. Tuczek, *Eur. J. Inorg. Chem.* **2018**, 1337–1355; d) Q. J. Bruch, G. P. Connor, N. D. McMillion, A. S. Goldman, F. Hasanayn, P. L. Holland, A. J. M. Miller, *ACS Catal.* **2020**, *10*, 10826–10846; e) M. J. Chalkley, M. W. Drover, J. C. Peters, *Chem. Rev.* **2020**, *120*, 5582–5636; f) G. Hochman, A. S. Goldman, F. A. Felder, J. M. Mayer, A. J. M. Miller, P. L. Holland, L. A. Goldman, P. Manocha, Z. Song, S. Aleti, *ACS Sustainable Chem. Eng.* **2020**, *8*, 8938–8948; g) G. Qing, R. Ghazfar, S. T. Jackowski, F. Habibzadeh, M. M. Ashtiani, C.-P. Chen, M. R. Smith, T. W. Hamann, *Chem. Rev.* **2020**, *120*, 5437–5516; h) D. Singh, W. R. Buratto, J. F. Torres, L. J. Murray, *Chem. Rev.* **2020**, *120*, 5517–5581; i) Y. Ashida, Y. Nishibayashi, *Chem. Commun.* **2021**, *57*, 1176–1189; j) S. J. K. Forrest, B. Schluschaß, E. Y. Yuzik-Klimova, S. Schneider, *Chem. Rev.* **2021**, *121*, 6522—6587; k) F. Masero, M. A. Perrin, S. Dey, V. Mougel, *Chem. Eur. J.* **2021**, *27*, 3892–3928; l) Y. Tanabe, Y. Nishibayashi, *Chem. Soc. Rev.* **2021**, *50*, 5201–5242.

[4] T. J. Hebden, R. R. Schrock, M. K. Takase, P. Müller, *Chem. Commun.* **2012**, *48*, 1851–1853.

[5] a) K. Arashiba, Y. Miyake, Y. Nishibayashi, *Nat. Chem.* **2011**, *3*, 120–125; b) S. Kuriyama, K. Arashiba, K. Nakajima, H. Tanaka, N. Kamaru, K. Yoshizawa, Y. Nishibayashi, *J. Am. Chem. Soc.* **2014**, *136*, 9719–9731; c) H. Tanaka, K. Arashiba, S. Kuriyama, A. Sasada, K. Nakajima, K. Yoshizawa, Y. Nishibayashi, *Nat. Commun.* **2014**, *5*, 3737; d) K. Arashiba, E. Kinoshita, S. Kuriyama, A. Eizawa, K. Nakajima, H. Tanaka, K. Yoshizawa, Y. Nishibayashi, *J. Am. Chem. Soc.* **2015**, *137*, 5666–5669; e) A. Eizawa, K. Arashiba, H. Tanaka, S. Kuriyama, Y. Matsuo, K. Nakajima, K. Yoshizawa, Y. Nishibayashi, *Nat. Commun.* **2017**, *8*, 4874; f) Y. Ashida, K. Arashiba, K. Nakajima, Y. Nishibayashi, *Nature* **2019**, *568*, 536–540; g) K. Arashiba, H. Tanaka, K. Yoshizawa, Y. Nishibayashi, *Chem. Eur. J.* **2020**, *26*, 13383–13389; h) Y. Tanabe, Y. Sekiguchi, H. Tanaka, A. Konomi, K. Yoshizawa, S. Kuriyama, Y. Nishibayashi, *Chem. Commun.* **2020**, *56*, 6933–6936.

[6] a) G. A. Silantyev, M. Förster, B. Schluschaß, J. Abbenseth, C. Würtele, C. Volkmann, M. C. Holthausen, S. Schneider, *Angew. Chem. Int. Ed.* **2017**, *56*, 5872–5876; *Angew. Chem.* **2017**, *129*, 5966–5970; b) J. Abbenseth, J.-P. H. Oudsen, B. Venderbosch, S. Demeshko, M. Finger, C. Herwig, C. Würtele, M. C. Holthausen, C. Limberg, M. Tromp, S. Schneider, *Inorg. Chem.* **2020**, *59*, 14367–14375.

[7] a) Q. Liao, N. Saffon-Merceron, N. Mézailles, *ACS Catal.* **2015**, *5*, 6902–6906; b) Q. Liao, A. Cavaillé, N. Saffon-Merceron, N. Mézailles, *Angew. Chem. Int. Ed.* **2016**, *55*, 11212–11216; *Angew. Chem.* **2016**, *128*, 11378–11382; c) M. F. Espada, S. Bennaamane, Q. Liao, N. Saffon-Merceron, S. Massou, E. Clot, N. Nebra, M. Fustier-Boutignon, N. Mézailles, *Angew. Chem. Int. Ed.* **2018**, *57*, 12865–12868; *Angew. Chem.* **2018**, *130*, 13047–13050; d) S. Bennaamane, M. F. Espada, A. Mulas, T. Personeni, N. Saffon-Merceron, M. Fustier-Boutignon, C. Bucher, N. Mézailles, *Angew. Chem. Int. Ed.* **2021**, *60*, 20210–20214; *Angew. Chem.* **2021**, *133*, 20372–20376.

 © 2021 The Authors. Angewandte Chemie International Edition published by Wiley-VCH GmbH

[8] J. Song, Q. Liao, X. Hong, L. Jin, N. Mézailles, *Angew. Chem. Int. Ed.* **2021**, *60*, 12242 – 12247; *Angew. Chem.* **2021**, *133*, 12350 – 12355.
[9] For recent reviews on the synthesis of *N*-containing products directly from N_2, see: a) S. Kim, F. Loose, P. J. Chirik, *Chem. Rev.* **2020**, *120*, 5637 – 5681; b) Z.-J. Lv, J. Wei, W.-X. Zhang, P. Chen, D. Deng, Z.-J. Shi, Z. Xi, *Natl. Sci. Rev.* **2020**, *7*, 1564 – 1583.
[10] R. Kalescky, E. Kraka, D. Cremer, *J. Phys. Chem. A* **2013**, *117*, 8981 – 8995.
[11] See Supporting Information for synthetic, computational and crystallographic details. Deposition numbers 2103549, 2103550, 2103551, 2103542, 2103553, 2103554, 2103555, 2103556 and 2103557 contain the supplementary crystallographic data for this paper. These data are provided free of charge by the joint Cambridge Crystallographic Data Centre and Fachinformationszentrum Karlsruhe Access Structures service.
[12] a) P. B. Winston, S. J. N. Burgmayer, T. L. Tonker, J. L. Templeton, *Organometallics* **1986**, *5*, 1707 – 1715; b) J. L. Templeton, in *Adv. Organomet. Chem.*, *Vol. 29* (Eds.: F. G. A. Stone, R. West), Academic Press, San Diego, **1989**, pp. 1 – 100.
[13] See Supporting Information for NEVPT2-CASSCF calculations for **1** and **2** and for a computational comparison to related ligand scaffolds and their Mo complexes.
[14] DFT calculations indicate that derivatives of **6** with one or two additional (terminal) N_2 ligands do not play a role (see Supporting Information). The anion of **5** was also considered as a possible intermediate, but no evidence for its formation was found upon reduction of **1** with excess Na/Pb at −20 °C.
[15] a) C. B. Powell, M. B. Hall, *Inorg. Chem.* **1984**, *23*, 4619 – 4627; b) M. D. Fryzuk, T. S. Haddad, M. Mylvaganam, D. H. McConville, S. J. Rettig, *J. Am. Chem. Soc.* **1993**, *115*, 2782 – 2792; c) I. Klopsch, E. Y. Yuzik-Klimova, S. Schneider, in *Nitrogen Fixation* (Ed.: Y. Nishibayashi), Springer Publishing, Berlin, **2017**, pp. 71 – 112; d) B. M. Lindley, R. S. van Alten, M. Finger, F. Schendzielorz, C. Würtele, A. J. M. Miller, I. Siewert, S. Schneider, *J. Am. Chem. Soc.* **2018**, *140*, 7922 – 7935.
[16] The calculated thermodynamic data show a considerable functional dependence with PBE affording the best results (see Supporting Information). A similar functional dependence has been reported recently for a N_2-bridged tungsten dimer, see: B. Schluschaß, J.-H. Borter, S. Rupp, S. Demeshko, C. Herwig, C. Limberg, N. A. Maciulis, J. Schneider, C. Würtele, V. Krewald, D. Schwarzer, S. Schneider, *JACS Au* **2021**, *1*, 879 – 894.
[17] R. A. Eikey, M. M. Abu-Omar, *Coord. Chem. Rev.* **2003**, *243*, 83 – 124.
[18] a) J. J. Curley, E. L. Sceats, C. C. Cummins, *J. Am. Chem. Soc.* **2006**, *128*, 14036 – 14037; b) J. S. Figueroa, N. A. Piro, C. R. Clough, C. C. Cummins, *J. Am. Chem. Soc.* **2006**, *128*, 940 – 950; c) I. Klopsch, M. Kinauer, M. Finger, C. Würtele, S. Schneider, *Angew. Chem. Int. Ed.* **2016**, *55*, 4786 – 4789; *Angew. Chem.* **2016**, *128*, 4864 – 4867; d) I. Klopsch, F. Schendzielorz, C. Volkmann, C. Würtele, S. Schneider, *Z. Anorg. Allg. Chem.* **2018**, *644*, 916 – 919.
[19] Related C–C coupling reactions have been reported, see for example: a) R. Duchateau, A. J. Williams, S. Gambarotta, M. Y. Chiang, *Inorg. Chem.* **1991**, *30*, 4863 – 4866; b) Y.-C. Tsai, M. J. A. Johnson, D. J. Mindiola, C. C. Cummins, W. T. Klooster, T. F. Koetzle, *J. Am. Chem. Soc.* **1999**, *121*, 10426 – 10427; c) J. J. Curley, T. Murahashi, C. C. Cummins, *Inorg. Chem.* **2009**, *48*, 7181 – 7193; d) L. Becker, P. Arndt, H. Jiao, A. Spannenberg, U. Rosenthal, *Angew. Chem. Int. Ed.* **2013**, *52*, 11396 – 11400; *Angew. Chem.* **2013**, *125*, 11607 – 11611.
[20] a) Other oxidants, such as $(^t\mathrm{BuNO})_2$ or TEMPO, also led to the formation of **11**, albeit in lower conversions; b) the reactions between **10**, MeCN and an oxidant (to afford **11**) was observed in thf as well; c) in the absence of **10**, no fumaronitril formation was noticed upon treatment of MeCN with the latter oxidants at 60 °C for 3d; d) *p*-chloranil is not suited as an oxidant, that is, no reaction between **10**, MeCN and chloranil was observed at 60 °C over the course of 3d.
[21] Upon reaction between **10**, AgOTf and PhCN in thf, the benzonitrile adduct of **10** was obtained as its triflate salt (see Supporting Information), indicating that the proposed coordination of MeCN is indeed feasible.

Manuscript received: August 21, 2021
Revised manuscript received: September 22, 2021
Accepted manuscript online: October 7, 2021
Version of record online: November 3, 2021

 © 2021 The Authors. Angewandte Chemie International Edition published by Wiley-VCH GmbH